Earth Surface Processes and Landforms
Earth Surf. Process. Landforms **24**, 809–824 (1999)

DRAINAGE DENSITY ON PROGRESSIVELY TILTED SURFACES WITH DIFFERENT GRADIENTS, WHEELER RIDGE, CALIFORNIA

PETER J. TALLING* AND MATTHEW J. SOWTER
Department of Geology, Bristol University, Queens Road, BS8 1RJ, UK

Received 10 November 1997; Revised 19 January 1999; Accepted 1 March 1999

ABSTRACT

Wheeler Ridge in the Southern San Joaquin Valley, California, is an anticlinal fold which has been progressively uplifted during the last 250 ka. Drainage networks on the ridge become younger as the anticline's eastern tip is approached. Because of the fold's asymmetric shape, surfaces on opposite flanks of the ridge have similar ages but very different gradients. The ridge provides important insights into drainage development on progressively tilted surfaces, as existing studies are restricted to static topography. A surface gradient of between 4·8° and *c.*10° is needed to initiate channel networks. This gradient threshold is consistent with previous studies of the gradient and upslope area needed to incise a channel through overland flow. Comparison of coeval drainage networks on opposite flanks of the ridge allows the controversial relationship between drainage density and gradient to be investigated. A lower valley density is observed on the higher gradient flank of Wheeler Ridge. Field observations from the ridge indicate that this inverse relationship is associated with hillslope erosion by shallow mass-wasting, the rate of which increases rapidly as a threshold gradient is approached. Comparison of data from Wheeler Ridge with other field studies and numerical models, shows that the form of the relationship between gradient and drainage density is process-dependent. A positive correlation occurs when erosion is a result of overland flow, whilst a negative correlation occurs where erosion is dominated by shallow mass-wasting.

KEY WORDS: drainage density; drainage evolution; slope; Wheeler Ridge; drainage initiation

INTRODUCTION

Drainage density is an important geometric parameter for channel networks as it determines the spacing of channels, the length of hillslopes, the maximum length-scale of slope failures, and reflects the processes governing landscape dissection (e.g. Schumm, 1997). The hydrological response of a channel network is strongly influenced by drainage density (Patten, 1988), and sediment erosion rates have been linked to channel spacing (Schumm, 1997). Numerous studies of relatively mature ($> c.100$ ka) landscapes have shown that drainage density is sensitive to climate (e.g. Gregory and Gardiner, 1975; Schumm, 1997), vegetation (e.g. Melton, 1958) and bedrock lithology (e.g. Schumm, 1997). There are few studies of how drainage density varies with time, although such studies provide important insights into the processes which determine drainage density. Previous work is restricted to flume-table experiments (Schumm *et al.*, 1987), and studies of landfills (Schumm, 1956), glacial tills (Ruhe, 1952), lava flows (Wells *et al.*, 1985), coastal terraces (Kashiwaya, 1987) and small areas of raised beach (Morisawa, 1964). Wheeler Ridge is an anticlinal fold in the hangingwall of an active thrust fault in the Southern San Joaquin Valley, California (Figures 1 and 2). Due to lateral propagation of the fault, drainage networks on the anticline are progressively younger as the fold's eastern tip is approached (Figures 1 and 2; Medwedeff, 1992; Keller *et al.*, 1998). The networks formed on surfaces underlain by a uniform lithology, and coeval networks experienced the same climatic fluctuations. These characteristics make the ridge a good location for studying the temporal evolution of drainage density.

The relationship between drainage density and gradient may also be investigated at Wheeler Ridge due to the fold's strongly asymmetric shape. Drainage networks on opposite flanks of the ridge have similar ages,

* Correspondence to: Dr P. J. Talling, Department of Earth Sciences, University of Bristol, Wills Memorial Building, Queens Road, Bristol, BS8 1RJ, UK. E-mail: peter.talling@bris.ac.uk

CCC 0197-9337/99/090809–16 $17.50

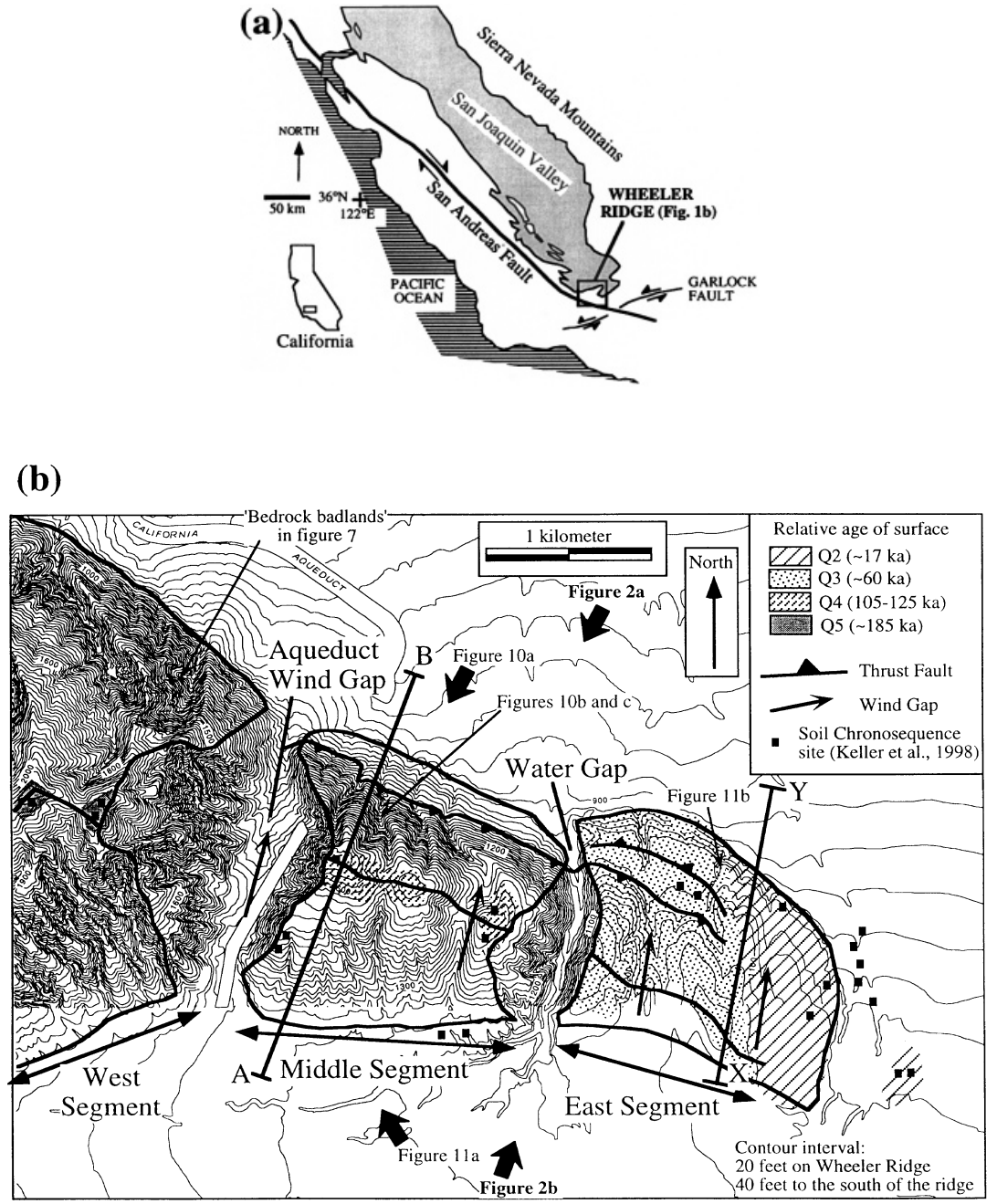

Figure 1. (a) Location of Wheeler Ridge at the southern end of the San Joaquin Valley, California. (b) Detailed topographic map showing the three segments that constitute the ridge. Surfaces dated by Keller *et al.* (1998) are shown, together with the location of emergent thrust faults (Mueller and Talling, 1997). The positions of topographic and structural cross-sections in Figure 5 are marked (A–B and X–Y), along with the locations of photographs shown in Figures 2, 7, 10 and 11

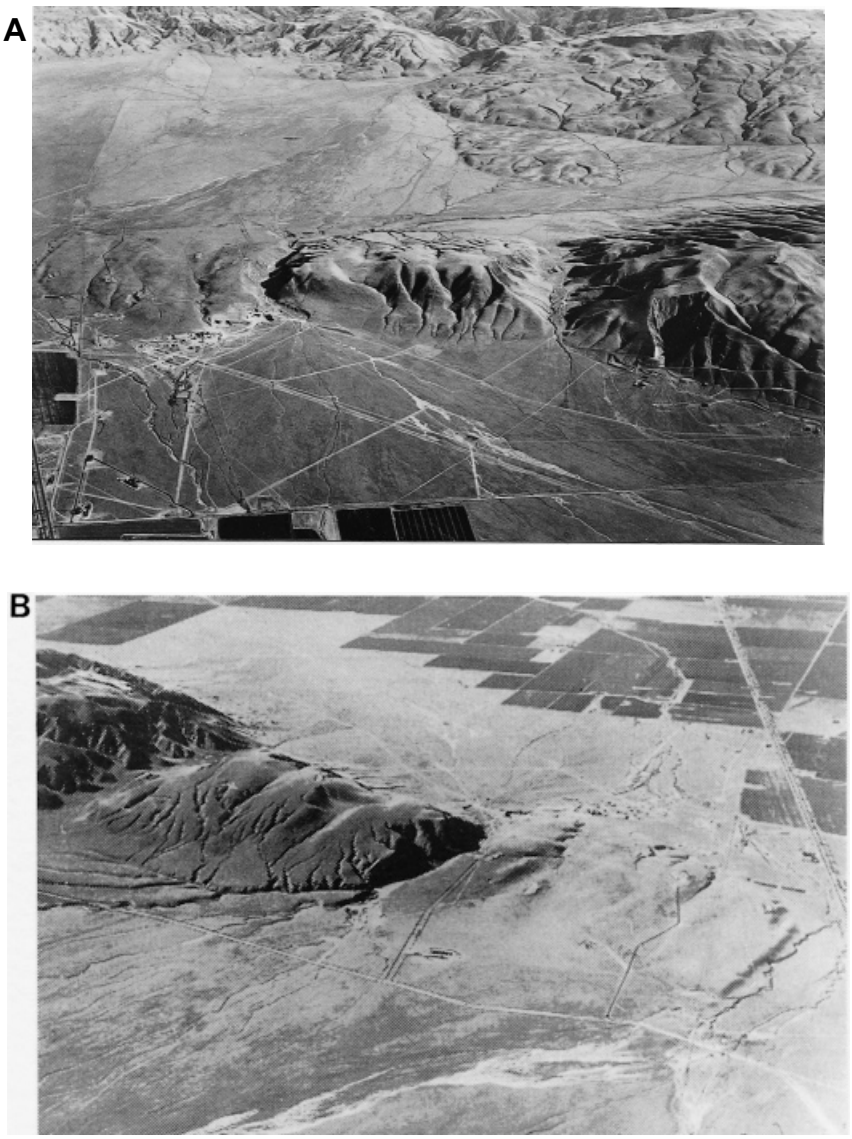

Figure 2. Aerial photographs of Wheeler Ridge courtesy of J. Shelton. (A) View looking south across the ridge. The water gap and wind gap, which now contains an aqueduct, divide the ridge into three segments (Figure 1b). The distance from water to wind gap is *c*. 1·5 km, and the middle segment of the ridge has *c*. 200 m of vertical relief (Figure 1b). A prominent area of bedrock, eroded into deep gullies, is visible just to the west of the wind gap. (B) View looking north across the ridge towards San Joaquin Valley. The I-5 freeway is visible near the ridge's eastern terminus

but formed on surfaces with very different gradients. The nature of this relationship is currently controversial (Oguchi, 1997). Field surveys in a number of different locations have shown that channel heads cut by overland flow are more closely spaced on steeper slopes (e.g. Dietrich *et al.*, 1992, 1993; Montgomery and Dietrich, 1994). This implies that drainage density will be higher on steeper slopes. However, field data from Japan (Oguchi, 1997), computer simulations (Howard, 1997; Tucker and Bras, 1998) and certain flume experiments (Mosley, 1974) indicate the presence of more widely spaced channels in areas of steeper surface gradients.

This study first documents how drainage density has evolved through time on Wheeler Ridge. The relationship between drainage density and slope is subsequently investigated, and it is shown that the form of this relationship depends upon the process which dominates hillslope erosion.

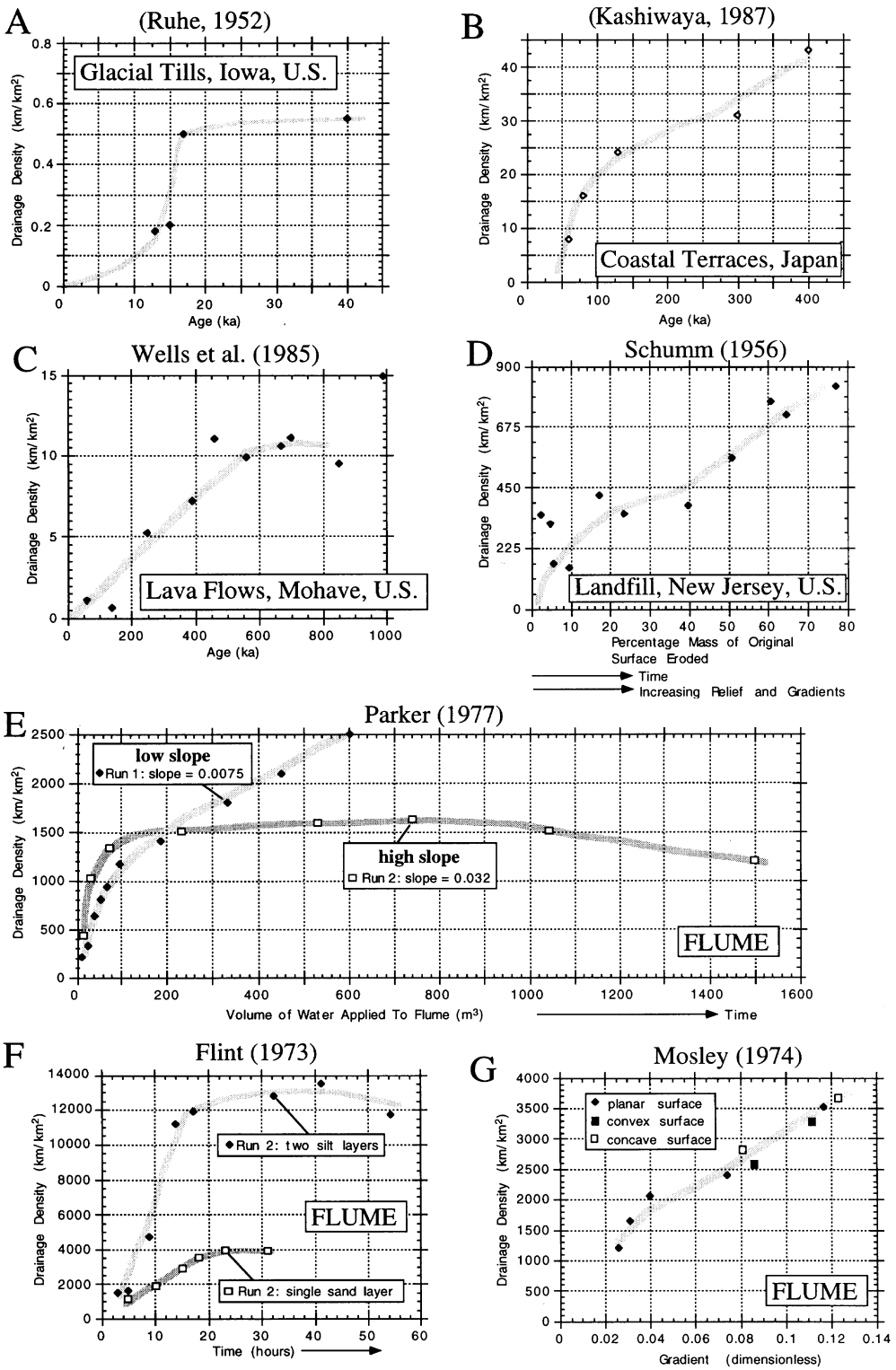

Figure 3. (A–D) Temporal evolution of drainage density on natural surfaces. (E, F) Temporal evolution of drainage density in flume experiments. (G) Relationship between surface gradient and drainage density observed in flume experiments

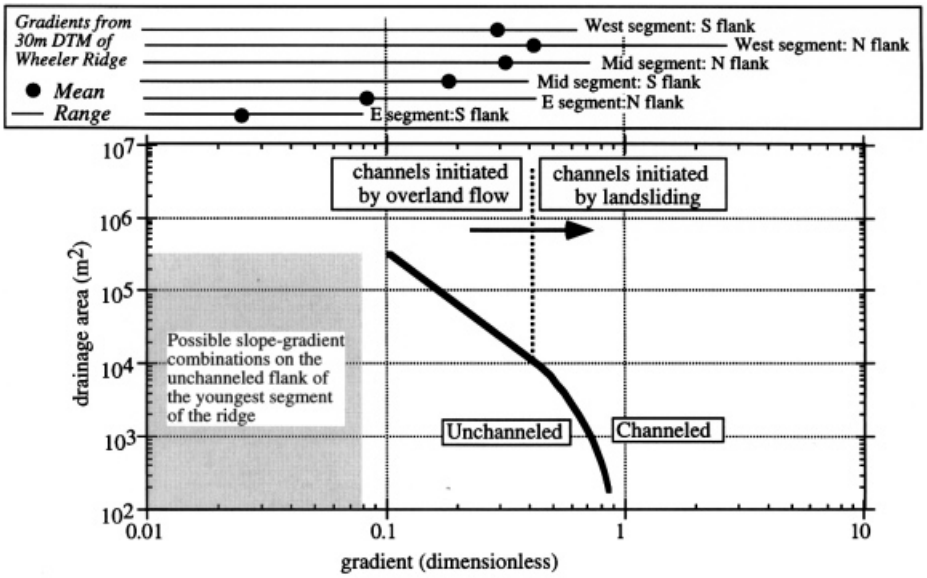

Figure 4. Relationship between local surface gradient, upstream drainage area, and presence or absence of channel heads (after Montgomery and Dietrich,(1994). A transition from channel heads cut by overland flow to channel heads cut by shallow landsliding is observed at a gradient of approximately 0·4 (Montgomery and Dietrich, 1994). The range of possible gradients and upslope drainage areas on the unchannelled flank of the youngest ridge segment is indicated in the shaded box. The mean (dot) and range of gradients for each surface is shown at the top of the figure. Gradients were derived using a 30 m resolution USGS digital terrain model

PREVIOUS WORK

Temporal evolution of drainage density

Studies of glacial tills (Ruhe, 1952) and lava flows (Wells *et al.*, 1985) initially show a rapid increase in drainage density, as the drainage network extends (Figure 3A, C). Drainage density subsequently reaches a constant value, although in both cases a single data point is crucial in defining such a trend (Figure 3A, C). This constant value has been interpreted as an equilibrium value for steady-state landscape (e.g. Howard, 1997). In contrast, data from coastal terraces (Kashiwaya, 1987) and short-term observation of a landfill (Schumm, 1956) do not show an equilibrium value (Figure 3B, D). This lack of an equilibrium value may be attributed to a short period of observation.

Small-scale drainage networks have been experimentally created on loose sediment using sprinkler systems to produce precipitation (Schumm *et al.*, 1987). Although such a technique allows the networks to be closely monitored, the processes responsible for network growth are not identical to those occurring on large-scale natural surfaces such as Wheeler Ridge. Complete overtopping of valley divides by water is unlikely to occur in large-scale valley networks, whilst it can cause drainage capture in the flume experiments. Both the experiments of Parker (1977) and Flint (1973) show that drainage density stabilizes after an initial period of rapid increase (Figure 3E, F). A slight decrease in drainage density is observed in the latter part of their experiments. Flint's work illustrates the importance of substrate lithology (Figure 3F). In Parker's experiments, a lower equilibrium drainage density is reached more rapidly on the higher gradient surface (Figure 3E).

Drainage density and gradient

Detailed field surveys in relatively low-gradient areas (slopes of $<c.$ 0·4) have shown that the gradient at a channel head is inversely related to the upslope contributing area (Montgomery and Dietrich, 1994; Dietrich *et al.*, 1992, 1993; Figure 4). As a smaller contributing area is needed to form a channel head on a steeper

slope, this relationship implies that there is a positive correlation between drainage density and surface gradient. However, field data from mountainous areas in Japan show that drainage density decreases as the dispersion of elevation increases (Oguchi, 1997). As elevation dispersion is positively correlated with surface gradient, this indicates a contrasting inverse relationship. Oguchi (1997) attributes this discrepancy to the relative importance of different processes of hillslope erosion, with the relationship seen in Japan reflecting the dominance of shallow mass-wasting. Computational models in which shallow mass-wasting (whose rate increases rapidly as a slope threshold is approached) dominates erosion show an inverse relationship between drainage density and elevation dispersion (Howard, 1997; Tucker and Bras, 1998). Different flume experiments also show contrasting relationships between drainage density and surface slope. Mosley (1974) documents a strong positive correlation on a series of planar, concave and convex surfaces (Figure 3G). The higher drainage density in Parker's two experiments, however, occurred on the lower-gradient surface (Figure 3E; Parker, 1977). Schumm's 1956 study of a landfill has been used to support a positive relationship between gradient and drainage density although the drainage density increases he observed may be attributed to increasing network age, rather than surface gradient (Figure 3D).

STUDY AREA

Wheeler Ridge is located at the southern end of the San Joaquin Valley in central California (Figures 1 and 2). The ridge exhibits up to 350 m of topographic relief and extends for *c*. 10 km along strike. The ridge was progressively uplifted by folding in the hangingwall of the Wheeler Ridge thrust (Medwedeff, 1992; Mueller and Talling, 1997). An unusually detailed interpretation of the subsurface thrust geometry was provided by Medwedeff (1992) based upon correlation of closely spaced subsurface data. The segment of the ridge between the wind and water gaps (Figures 1 and 2) was formed above a wedge thrust (Figure 5). This interpretation accounts for an upward increase in structural relief within the fold, indicating the presence of a second south-vergent thrust ramp, and a lack of obvious thrust-related shortening north of Wheeler Ridge. Another south-dipping thrust offsets strata in the uppermost part of the fold (Medwedeff, 1992). This fault outcrops along part of the fold's northern flank, producing a sharp break in slope (Figure 1b; Mueller and Talling, 1997). Near the eastern termination of the ridge this latter fault and the upper surface of the wedge-thrust are absent, resulting in a simpler fault geometry (Figures 1b and 5). Subsurface and geomorphic evidence shows that a series of vertical tear faults oriented perpendicular to the ridge crest coincide with the position of wind and water gaps (Medwedeff, 1992; Mueller and Talling, 1997; Keller *et al.*, 1998). Bedrock consists of conglomeratic sandstone with predominantly granitic clasts (Davis, 1983; Medwedeff, 1992; Keller *et al.*, 1998). These strata are often poorly consolidated and range from the Plio-Pleistocene (Tulare Formation) to recent in age, with good exposures occurring in both wind and water gaps (Figures 1 and 2; Keller *et al.*, 1998).

Uplifted depositional surfaces are well preserved on both flanks of the ridge (Figure 2). Soil chronosequences based upon rubification, and the abundance of clay or carbonate, have unambiguously shown that surfaces near the ridge crest become progressively younger towards the east (Figure 1b; Keller *et al.*, 1998). Thus, although the slip direction of the thrust is towards the north, lateral migration of the fault's tip has resulted in the eastward migration of the fold (Medwedeff, 1992). Absolute dating of these surfaces is based on two radiocarbon dates (Keller *et al.*, 1998). A sample of detrital charcoal indicates that a relatively undeformed alluvial fan surface, lying to the east of the water gap at the ridge's eastern terminus, is less than 7 ka in age. Pedogenic carbonate rinds on gravel clasts yield an age of 9 ± 3 ka for the eastern end of the eastern segment of the ridge (Figure 1b). It is estimated that *c*. 5 ka is needed to form such rinds (Seaver, 1986), and an age of 14 ± 3 ka is determined for the eastern part of the eastern ridge-segment (Figure 1b). Owing to a lack of further absolute dates, the ages of surfaces further to the west are estimated by assuming that uplift rates remained constant. Soil ages derived from these estimates are consistent with well dated soil chronosequences in the northern San Joaquin Valley (Keller *et al.*, 1998). Surfaces on the upper parts of opposite flanks of the ridge are the same age, but due to the asymmetric shape of the anticline they have significantly different gradients (Figure 5; Table I). Ongoing uplift has progressively rotated and steepened surfaces on the ridge (Figure 5). A factor which complicates this pattern is the emergent thrust fault which outcrops along the

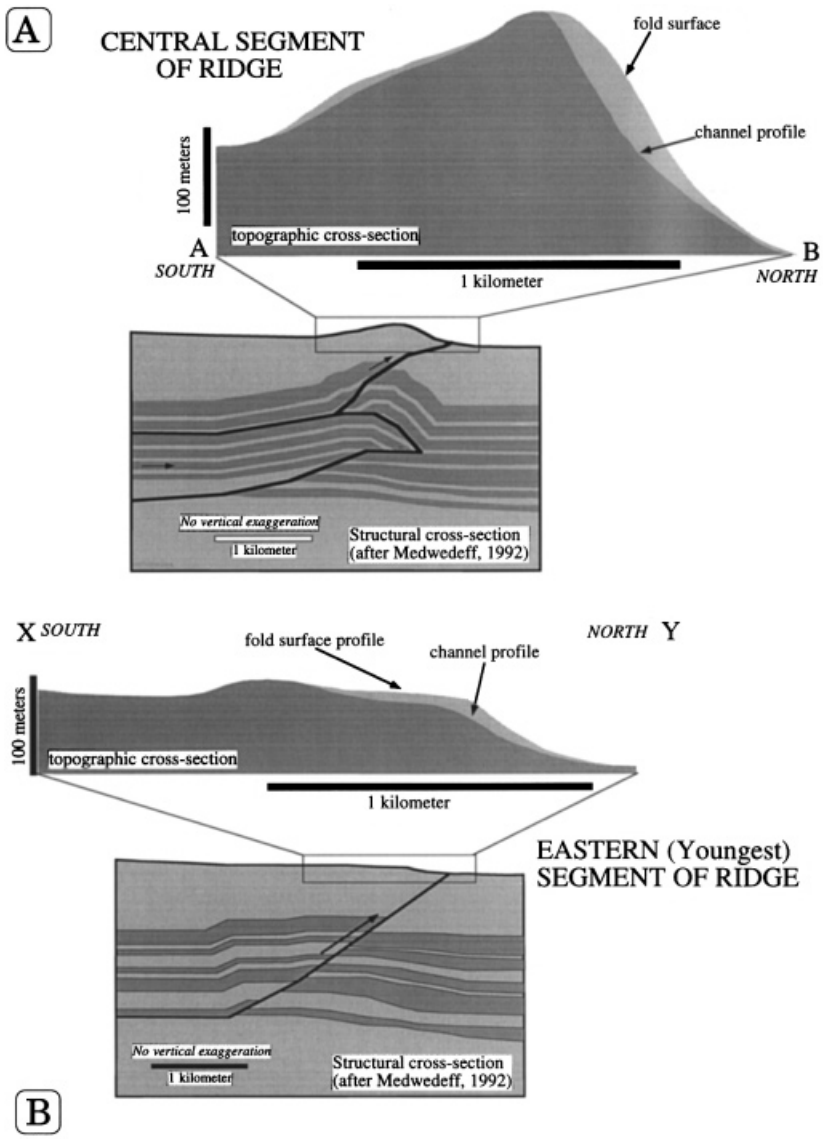

Figure 5. Structural and topographic cross-sections across (A) the central part of the ridge and (B) the eastern (youngest) part of the ridge. The exact locations are indicated in Figure 1b. Structural cross-sections are after Medwedeff (1992). Channel profiles have been projected onto the topographic profiles, which closely approximate the undissected shape of the fold

ridge's northern flank (Figure 1b). Surfaces on the northern flank which lie on opposite sides of this fault have slightly different ages, as uplift to the north of the fault is relatively recent (Mueller and Talling, 1997).

The ridge currently has an arid to semi-arid climate, with an average annual precipitation of 150 mm. Ninety per cent of this precipitation occurs between October and April (Soil Conservation Service, 1988; Keller *et al.*, 1998). Summer temperatures often reach 38°C and rarely fall below 30°C. During the winter months temperatures can regularly fall below freezing (Keller *et al.*, 1998). Climates during the previous *c.* 250 ka will have changed dramatically. The area was significantly wetter and cooler during glacial periods, such as that between 85 and 10 ka (Smith *et al.*, 1997; Davis and Coplen, 1989). Pollen records show that pinyon and juniper woodland was present in the northern part of the San Joaquin valley during this period, indicating an annual precipitation of *c.* 350–500 mm (Davis and Coplen, 1989). Such an increase in

Table I. Drainage density and morphometric parameters for surfaces on Wheeler Ridge

Surface location	Age (ka)	Area (km^2)	Map drainage density (km^{-1})	Air photo drainage density (km^{-1})	Gradient (mean)	Gradient (std dev.)	Gradient (max.)	Mean channel sinuosity
East Segment								
South flank	17–60	0·294	0	0	0·02	0·02	0·08	
North flank		1·007	4·33	3·55	0·09	0·06	0·43	
Middle Segment								
South flank	105–125	0·939	7·32	10·68	0·19	0·07	0·41	1·06
North Flank (all)		0·779	4·60	7·08	0·31	0·15	0·78	1·03
North Flank (above fault)		0·555	4·29	5·09				
West Segment								
South flank	*c.* 185	1·997	7·50	11·47	0·26	0·11	0·67	
North flank		2·242	5·65	9·60	0·41	0·16	1·17	

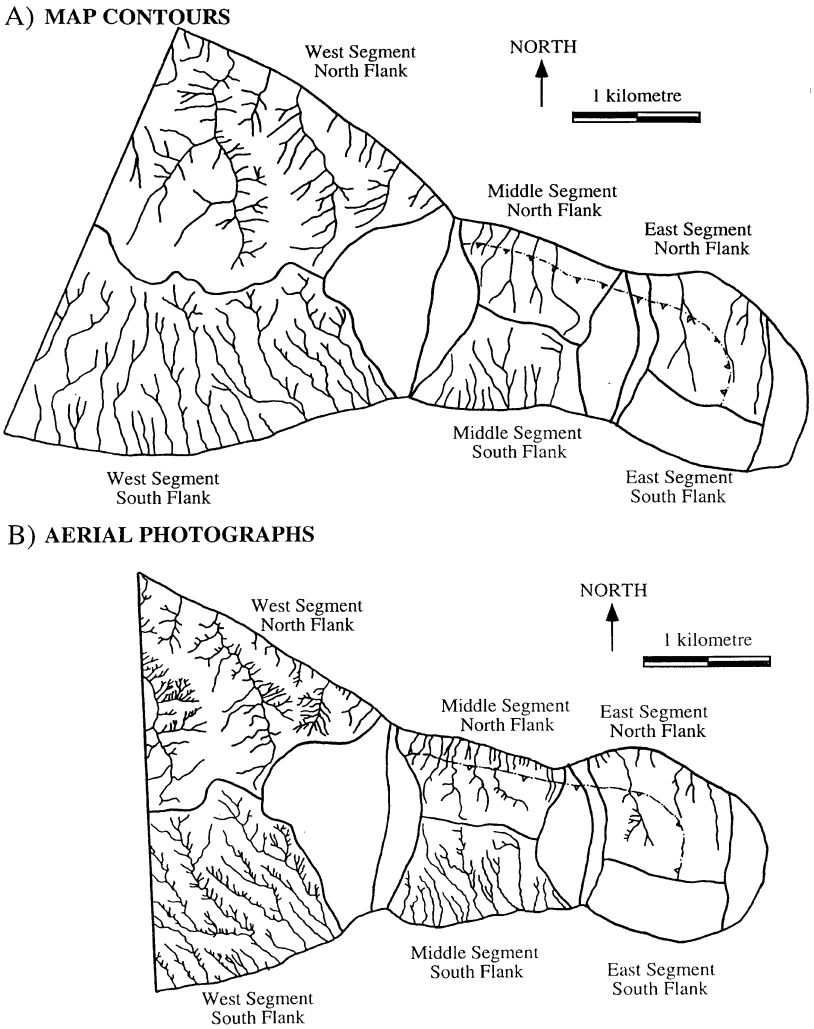

Figure 6. Drainage networks defined by (A) 1:24 000 topographic map contour crenulations, and (B) 1:16 000 aerial photographs. The emergent thrust fault (Mueller and Talling, 1997) which was used to subdivide the northern flank of the ridge is marked by a barbed line

Figure 7. View of the steeper northern flank of the ridge on either side of the aqueduct wind gap. To the west of the wind gap an area of bedrock has been exposed, which has been deeply incised by numerous closely spaced gullies. This area of bedrock badlands is also clearly visible on Figure 2A. Similar 'bedrock badlands' occur on the flanks of the wind and water gaps, and in a few locations on the shallower southern flank of the western (oldest) ridge segment

precipitation may have substantially increased drainage densities (Gregory and Gardiner, 1975; Schumm, 1997). Fan aggradation events occurred in the region at 125, 55 and 10 ka, indicating periods of either more rapid erosion or lower runoff (Keller *et al.*, 1998).

METHOD

The way in which drainage density is measured has a significant effect on the values obtained (e.g. Table I; Gregory and Walling, 1972). Measurements may be made from topographic maps using streams ('blue lines') marked on by the cartographer or by inferring channels where contour lines are crenulated. The latter approach measures valley density rather than channel density (Montgomery and Dietrich, 1994), and may be affected by the scale of maps employed (Giusti and Schneider, 1962). Drainage density can be calculated by mapping channels, either in the field or on aerial photographs (Figure 6). More recently, digital terrain models have been used to define channel networks and drainage density (Dietrich *et al.*, 1992, 1993). This study delineated channel networks and channel heads using 1:16 000 scale aerial photographs purchased from the US Geological Survey (USGS) (Figure 6A), and using contour crenulations on 1:24 000 scale USGS topographic maps (Figure 6B). Field mapping showed that channel heads could be more accurately defined on aerial photographs, in comparison to maps or digital terrain models, for well vegetated, low-gradient parts of the ridge. However, in areas of predominantly bare rock characterized by very steep and highly incised 'badland' topography with very closely spaced channels, the aerial photographs were insufficient to identify the detailed channel network. Such areas occur primarily on the western part of the ridge and in the wind and water gaps (Figures 2 and 7). The extremely high drainage densities associated with these localized bedrock badlands complicate the relationship between gradient and drainage density observed elsewhere on the ridge. Channel drainage densities are also ephemerally effected by rapid migration of channel heads due to short-term climatic fluctuations (Bull and Kirkby, 1997), or road cuts (field observations, 1993). The use of valley densities is favoured in this study, as it minimizes both of these problems. Drainage densities on the flanks of the wind and water gaps were not included in this study because these locations are dominated by bedrock badlands.

RESULTS

Drainage densities of up to 12 km km^{-2} were measured on aerial photographs, whilst value of less than 8 km km^{-2} were obtained from contour crenulations (Figure 8 and Table I). A much greater number of first-order channels was observed on aerial photographs, although both methods determined a similar higher-order channel network.

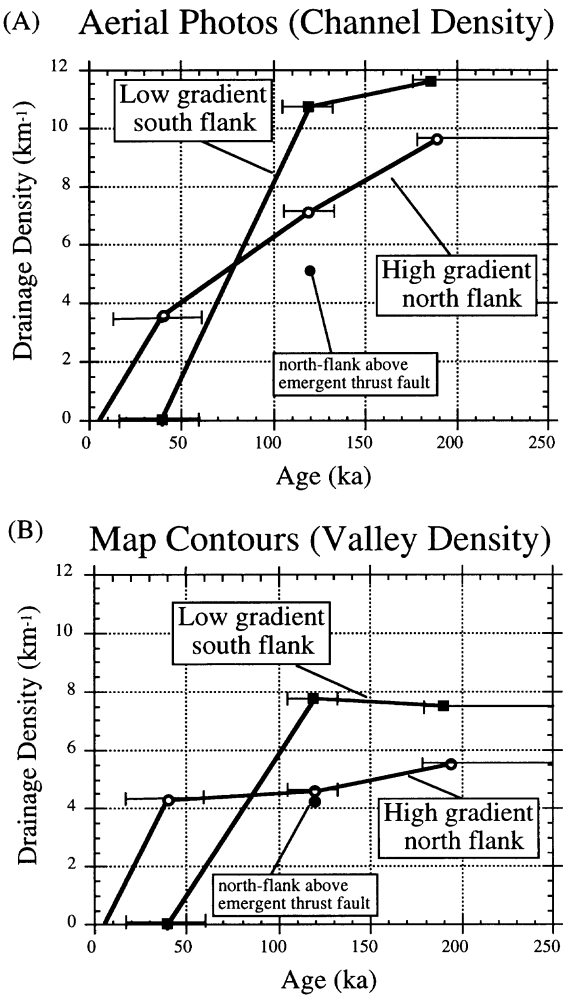

Figure 8. Temporal evolution of drainage density on either flank of Wheeler Ridge based on (A) aerial photographs, and (B) contour crenulations on topographic maps. Ages are from Keller *et al.* (1998). The northern flank of the middle ridge segment was subdivided using the position of an emergent thrust fault (Figure 6). Drainage densities on either side of this fault are indicated

Drainage density and time

As previously noted by Keller *et al.* (1998), a threshold slope of greater than 0·08 (4·8°) is needed to initiate channels on the eastern ridge segment (Figures 4 and 9; Table I). This is consistent with previous studies of channel head formation by overland flow. They have shown that if a channel head is to be cut, a threshold slope must be exceeded for a given upslope contributing area (Figure 4). If the data of Montgomery and Dietrich (1994) are extrapolated to relatively low slopes, the eastern ridge segment plots below the threshold for channel head cutting (Figure 4).

Near-constant valley densities were reached on the ridge's steeper northern flank after *c*. 40 ka, and within *c*. 80 ka of channel initiation on the shallower southern flank, although it must be stressed that *such trends depend on the position of single data points*. Channel densities continued to increase throughout the *c*. 200 ka period, most significantly on the steeper northern flank. These increases may be partly due to occasional development of bedrock badlands on the oldest segment of the ridge (Figure 1), and the absence of such badlands on the other surfaces considered in this study. The temporal evolution of drainage density on Wheeler Ridge may be compared with sparse data from other field locations and flume experiments (Figure

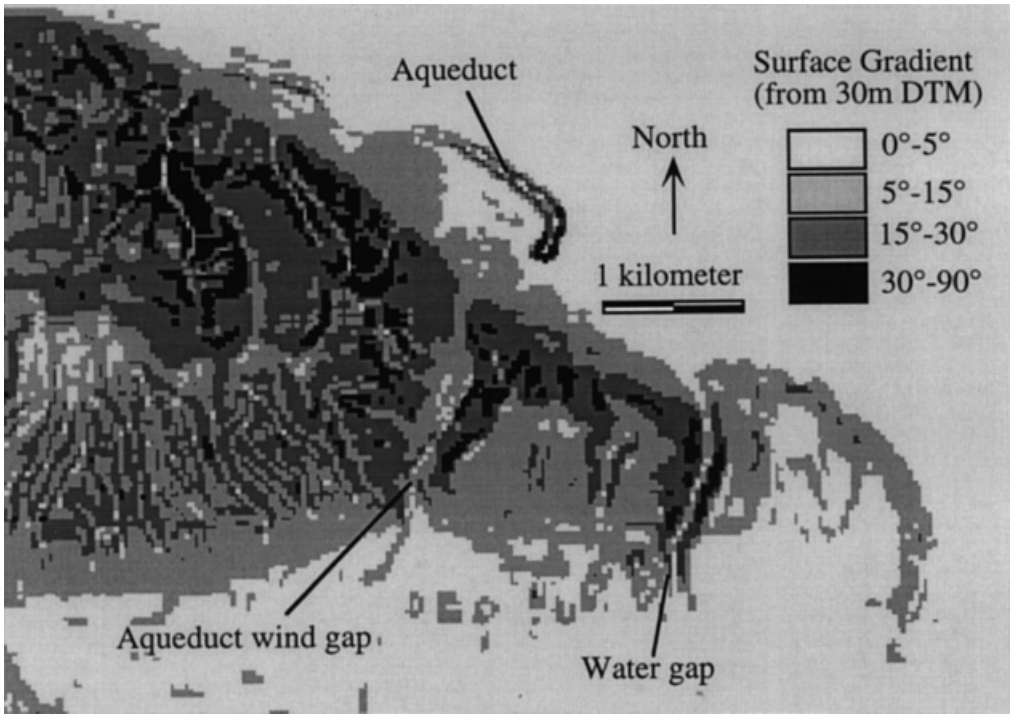

Figure 9. Map of surface gradients derived from 30 m resolution USGS digital elevation model. The area of high gradients to the north of the aqueduct wind gap is a man-made aqueduct. Shallow mass-wasting-prone slopes of $< 30^{\circ}$ (0·58) are located in gorges which traverse the ridge, and on the northern flank of the middle and western ridge segments. Note that gradients on the ground may locally exceed those portrayed in this 30 m resolution data set (Dietrich *et al.*, 1993)

3). An equilibrium valley density was reached after 10 ka on glacial tills, whilst on lava flows an equilibrium channel density was reached after *c*. 1 Ma (Figure 2; Ruhe, 1952; Wells *et al.*, 1985). This shows that the time taken to reach equilibrium may vary by two orders of magnitude, with longer periods characterizing more resistant lithologies. It must be noted again that such an interpretation is dependent on the position of a few data points (Figure 3A, C).

Drainage density and surface gradient

On Wheeler Ridge, a lower equilibrium valley density was reached more rapidly on the higher-gradient northern flank, once the threshold gradient for channel cutting was exceeded (Figure 8). A strikingly similar relationship is shown by the flume experiments of Parker (1977; Figure 3E). If surfaces on opposite sides of the middle ridge segment are compared, data from Wheeler Ridge support an inverse relationship between valley density and slope (Figure 8). Dinklage (1991) suggested that this relationship was due to the presence of more sinuous channels on the lower-gradient surface. Mean channel sinuosities were measured from the aerial photographs for surfaces on either flank of the middle ridge segment. An increase in sinuosity from 1·03 to 1·06 is insufficient to account for the observed variations in drainage density (Table I).

It is proposed that the relationship between surface gradient and drainage density depends upon the process controlling hillslope erosion and channel head cutting. On surfaces dominated by overland flow, the area upslope of channel heads is inversely related to gradient at the channel head (e.g. Montgomery and Dietrich, 1994). As the spacing of channel heads is determined by upslope area, this results in a positive correlation between drainage density and overall surface gradient. Once a threshold slope (*c*.0·4) is reached, shallow mass-wasting dominates hillslope erosion and channel head formation, and the position of channel heads becomes independent of upslope area (Figure 4; Montgomery and Dietrich, 1994; Dietrich *et al.*, 1992, 1993). Oguchi's (1997) field study in Japan illustrates how poorly defined gullies cut by shallow mass-wasting (his

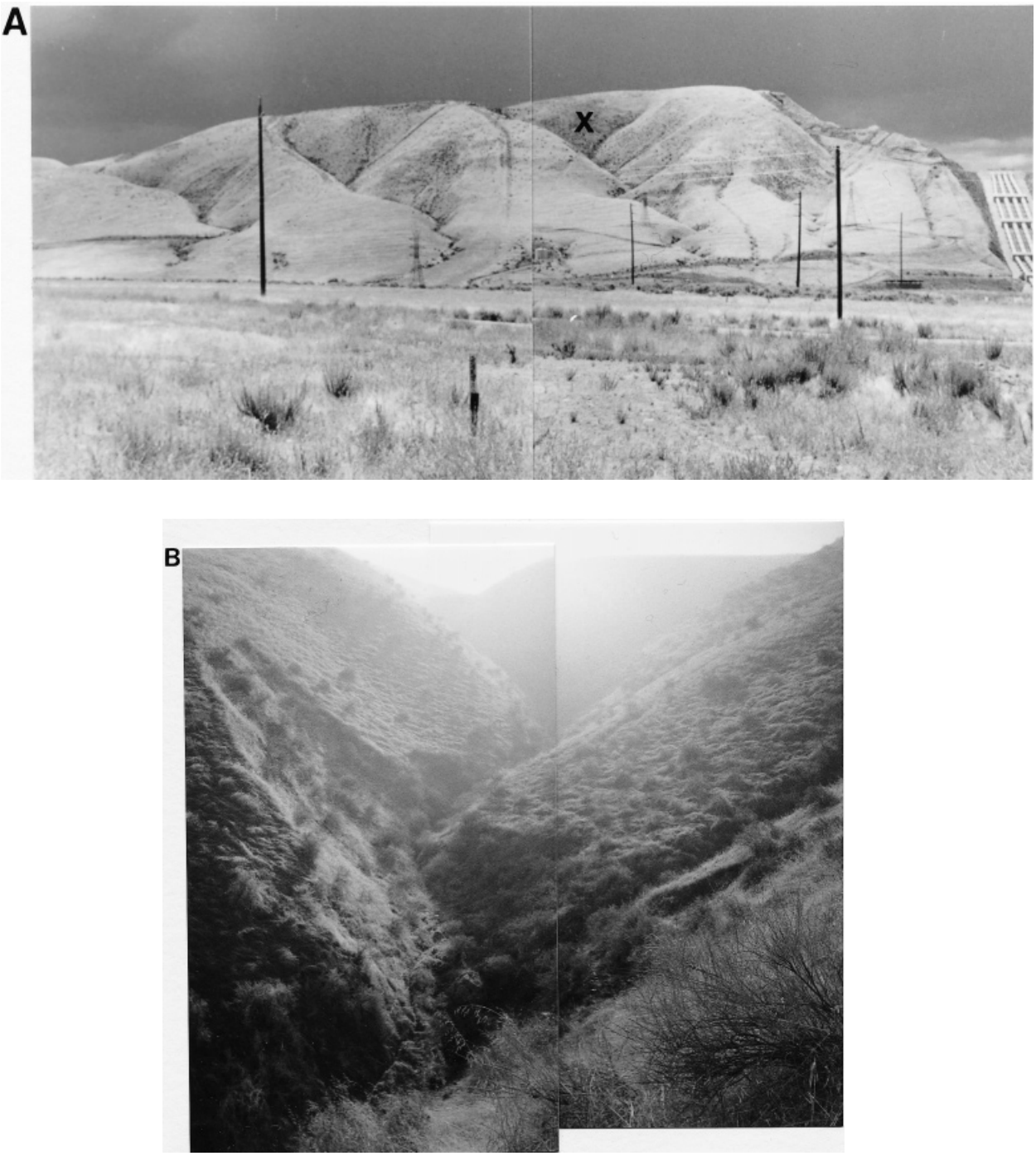

Figure 10.

Figure 10. (A) Photograph of the steeper northern flank of the middle ridge segment. The California Aqueduct, which runs through the Wind Gap, can be seen on the western side of the photograph. Maximum relief is *c*. 750 feet (*c*. 230 m) and the lateral extent of the photograph is *c*. 1 km. (B, C) Photographs of a drainage basin (marked X on Figure 10A) on the steeper northern flank of the ridge's middle segment. Undercutting of the hillslopes by channels is commonplace. A prominent 10 m high scar directly above the channel, at the base of the hillslope, is seen in both photographs. Note the steepness and rectilinear form of the hillslopes

S-type channels) are quickly removed by hillslope failure in adjacent locations. Such poorly defined gullies would not be recognizable as valleys using the contour crenulations method employed in this study (i.e. internal angle of *c*.20°). Howard (1994, 1997), Tucker and Bras (1998) and Roering *et al.* (1997) have numerically modelled landscape evolution dominated by threshold-slope dependent mass-wasting. In their models, hillslope erosion rates increase rapidly as the threshold slope is approached. Their models indicate that rectilinear hillslopes, whose gradient is near the threshold slope, are indicative of such mass-wasting (Anderson, 1994; Howard, 1994, 1997; Roering *et al.*, 1997; Tucker and Bras, 1998, figure 3). The inverse relationship between valley density and topographic gradient (measured from drainage outlet to divide or 90 per cent of distance along trunk channel) was reproduced by Howard's (1994) and Tucker and Bras' (1998) models. Tucker and Bras additionally observed that drainage density was positively correlated with relief when Hortonian overland flow dominated erosion, whilst for erosion by saturation-excess runoff a negative correlative occurred.

Field observations from Wheeler Ridge indicate that shallow mass-wasting is an important erosional process on the steeper parts of the ridge. Very steep hillslope gradients ($> 0{\cdot}58$ or 30°; Figures 9 and 10) on the northern flank of the middle ridge segment are similar to gradients documented in other areas of shallow mass-wasting (Table I, Figures 4 and 9; Montgomery and Dietrich, 1994). The rectilinear form of hillslopes on these steeper parts of the ridge (Figure 10) is indicative of threshold-gradient dependent mass-wasting. Lower-gradient hillslopes east of the water gap and on the southern flank of the ridge have convex–concave hillslope profiles, which reflect erosion by creep and overland flow (Figure 11; e.g. Carson and Kirkby, 1972).

The exact nature of mass-wasting processes on the very steep hillslopes of Wheeler Ridge could include shallow bedrock-involved landslide, regolith-only landsliding or less-catastrophic creep of the colluvial regolith that is non-linearly dependent on gradient. Undercutting of the base of slopes by channels is

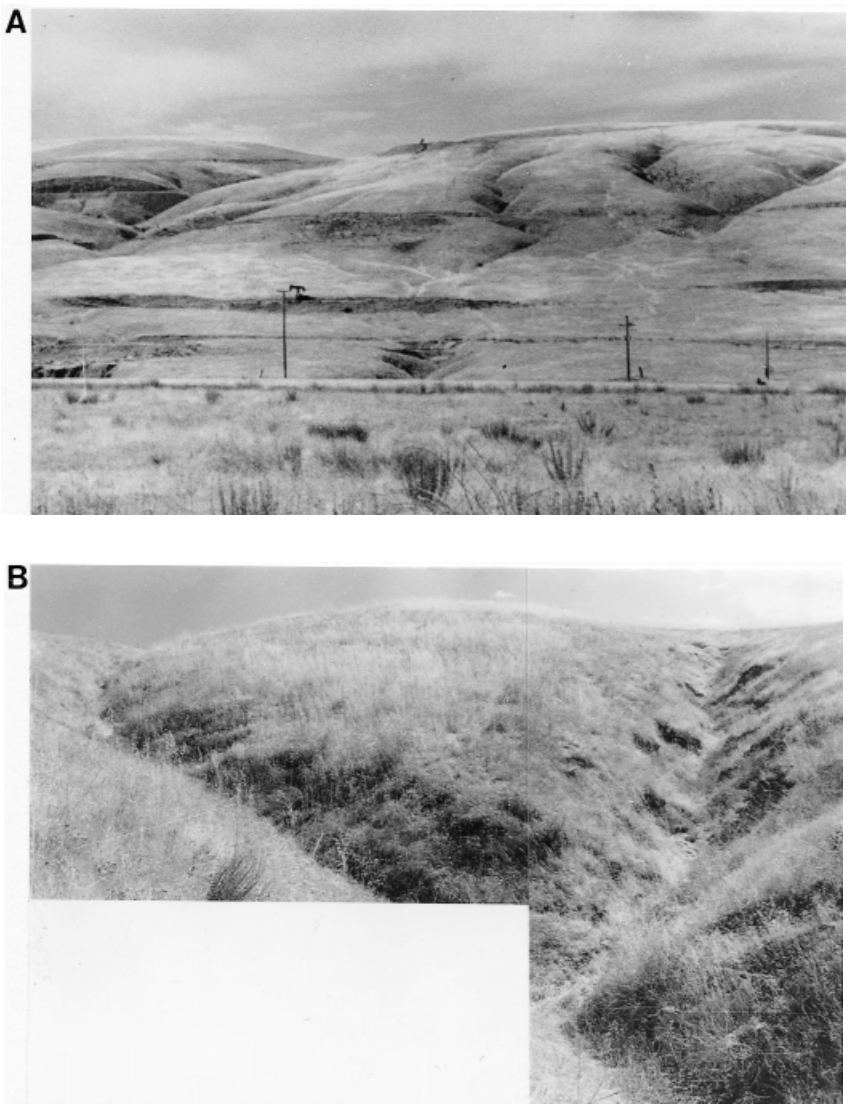

Figure 11. Photographs of lower-gradient hillslopes on (A) the southern flank of the middle ridge segment, and (B) the northern flank of the eastern (youngest) ridge segment (Figure 1b). The field of view in (A) is about 700 m wide and shows *c*. 120 m of relief. (B) shows an area that is *c*. 60 m wide. Channels locally undercut the hillslopes to form V-shaped cross-sections. Intervening hillslopes are convex–concave and approximate the undissected original shape of the fold

commonly observed and suggests that shallow bedrock-involved landsliding is important (Densmore *et al.*, 1997). However, fresh scars were not observed on the higher parts of the hillslopes. On these particularly steep slopes a shallow (*c*. 30 cm thick), poorly consolidated, colluvial regolith, derived from sandy conglomeratic bedrock, is held together by a thick mat of long grass. This regolith layer is prone to moving easily downslope under the weight of a person's feet. This observation supports the occurrence of regolith only landsliding or rapid creep.

The numerical models of Howard (1994, 1997) and Tucker and Bras (1998), in which hillslope erosion was dominated by threshold-dependent mass-wasting, intriguingly found that lower valley densities occurred when channel erosion rates were increased. Low valley densities on the steeper surfaces of Wheeler Ridge are also associated with rapid channel incision (Figures 5 and 8). The comparison between these numerical

models and Wheeler Ridge is likely to be inaccurate, however, because there is no field evidence that the lower-gradient hillslopes on Wheeler Ridge are undergoing erosion by mass-wasting (Figure 11).

CONCLUSIONS

A slope of greater than 4·8° is needed to initiate channel networks on the ridge (Keller *et al.*, 1998). This threshold is consistent with the relationships between slope and upstream area needed to initiate channels by overland flow (Montgomery and Dietrich, 1994). Near-constant valley densities are reached at Wheeler Ridge after 40–80 ka, once the channel network has been initiated. Lower equilibrium valley densities are developed more rapidly on surfaces with higher gradients, as observed in Parker's (1977) flume experiments. Data from the ridge, field studies in Japan (Oguchi, 1997), and computer models (Howard, 1994, 1997; Tucker and Bras, 1998) indicate that the negative correlation between drainage density and gradient is related to the dominance of erosion by shallow mass-wasting. In areas where erosion is dominated by overland flow a positive correlation between surface gradient and drainage density will occur.

REFERENCES

Anderson, R. S. 1994. 'Evolution of the Santa Cruz mountains, California, through tectonic growth and geomorphic decay', *Journal of Geophysical Research*, **99**, 20161–20181.

Bull, L. J. and Kirkby, M. J. 1997. 'Gulley processes and modelling', *Progress in Physical Geography*, **21**, 354–374.

Carson, M. A. and Kirkby, M. J. 1972. Hillslope Form and Process, Cambridge University Press, Cambridge.

Davis, T. L. 1983. Late Cenozoic structure and tectonic history of the western Big Bend of the San Andreas Fault and Adjacent San Emigdio Mountains, PhD Dissertation, University of California, Santa Barbara, 508 pp.

Davis, G. H. and Coplen, J. B. 1989. Late Cenozoic paleohydrology of the western San Joaquin Valley, California, as related to structural movements in the central Coast Ranges, Geological Society of America Special Publication, 234.

Densmore, A. L., Anderson, R. S., McAdoo, B. G. and Ellis, M. A. 1997. 'Hillslope erosion by bedrock landslides', *Science*, **275**, 369–372.

Dietrich, W. E., Wilson, C. J., Montgomery, D. R., McKean, J. and Bauer, R. 1992. 'Erosion thresholds and land surface morphology', *Geology*, **20**, 675–679.

Dietrich, W. E., Wilson, C. J., Montgomery, D. R. and McKean, J. 1993. 'Analysis of erosion thresholds, channel networks, and landscape morphology using a digital terrain model', *The Journal of Geology*, **101**, 259–278.

Dinklage, W. 1991. The evolution of drainage density on the Wheeler Ridge an active fault-bend-fold anticline, southern San Joaquin valley, Minor Comps. Paper, University of California, Santa Barbara.

Flint, J.-J. 1973. 'Experimental development of headward growth by channel networks', *Geological Society of America Bulletin*, **84**, 1087–1094.

Giusti, E. V. and Schneider, W. J. 1962. Comparison of drainage on topographic maps of the Piedmont province, United States Geological Survey Professional Paper, 450E.

Gregory, K. J. and Gardiner, V. 1975. 'Drainage density and climate', *Zeitschrift fur Geomorphologie N.F.*, **19**, 287–298.

Gregory, K. J. and Walling, D. E. 1973. Drainage Basin: Form and Process, Edward Arnold, London.

Howard, A. D. 1994. 'A detachment-limited model of drainage basin evolution', *Water Resources Research*, **30**, 2261–2285.

Howard, A. D. 1997. 'Badland morphology and evolution: Interpretation using a simulation model', *Earth Surface Processes*, **22**, 211–227.

Kashiwaya, K. 1987. 'Theoretical investigation of the time variation of drainage density', *Earth Surface Processes*, **12**, 39–46.

Keller, E. A., Zepeda, R. L., Rockwell, T. K. and Ku, T.-L. 1998. 'Active tectonics and soil chronology of Wheeler Ridge, Southern San Joaquin Valley, California', *Geological Society of America Bulletin*, **110**, 298–310.

Medwedeff, D. A. 1992. 'Geometry and kinematics of an active, laterally propagating wedge thrust, Wheeler Ridge, California', in Mitra, S. and Fisher, G. W. (Eds), Structural Geology of Fold and Thrust Belts, 1–28.

Melton, M. A. 1958. 'Geometric properties of mature drainage systems in E4 phase space', *Journal of Geology*, **66**, 35–54.

Montgomery, D. R. and Dietrich, W. E. 1994. 'Landscape dissection and drainage area-slope thresholds' in Process Models in Theoretical Geomorphology, Wiley, New York.

Morisawa, M. E. 1964. 'Development of drainage systems on an upraised lake floor', *American Journal of Science*, **262**, 340–354.

Mosley, M. P. 1974. 'An experimental study of rill erosion', *Transactions of the American Society of Agricultural Engineers*, **68**, 909–916.

Mueller, K. and Talling, P. J. 1997. 'Geomorphic evidence for tear faults accommodating lateral propagation of an active fault-bend fold, Wheeler Ridge, California', *Journal of Structural Geology*, **19**, 397–411.

Oguchi, T. 1997. 'Drainage density and relative relief in humid steep mountains with frequent slope failure', *Earth Surface Processes*, **22**, 107–120.

Parker, R. S. 1977. Experimental study of drainage basin evolution and its hydrological implications, Colorado State University Hydrology Papers, 90, Fort Collins, Colorado.

Patten, P. C. 1988. 'Drainage basin morphometry and floods', in Baker, V. C., Kochel, R. C. and Patton P. C., (Eds), Flood Geomorphology, Wiley, New York.

Roering, J. J., Kirschner, J. W. and Dietrich, W. E. 1997. 'Evidence for a non-linear diffusive mass wasting transport law and

implications for hillslope evolution in the Oregon Coast Range', *Eos: Transactions of the American Geophysical Union*, **78**, F287.
Ruhe, R. V. 1952. 'Topographic discontinuities of the Des Moines Lobe', *American Journal of Science*, **250**, 46–56.
Schumm, S. A. 1956. 'The evolution of drainage systems and slopes in badlands at Perth Amboy, New Jersey', *Bulletin of the Geological Society of America*, **67**, 597–646.
Schumm, S. A. 1997. 'Drainage density: Problems of prediction' in Stoddart, D. R. (Ed.), Process and Form in Geomorphology, Routledge, London.
Schumm, S. A., Mosley, M. P. and Weaver, W. E. 1987. Experimental Fluvial Geomorphology, Wiley-Interscience, New York.
Seaver, D. B. 1986. Quaternary evolution and deformation of the San Emigdio Mountains and their alluvial fans, Transverse Ranges, California, MA thesis, University of California, Santa Barbara.
Smith, G. I., Bischoff, J. L. and Bradbury, J. P. 1997. 'Synthesis of the paleoclimatic record from Owens Lake core OL-92', in An 80,000-year Paleoclimatic Record from Owens Lake, California, Geological Society of America Special Publication, 317, 143–161.
Soil Conservation Service. 1988. Soil survey of Kern County, California, northwestern part, US Department of Agriculture, 304 pp.
Tucker, G. E. and Bras, R. L. 1998. 'Hillslope processes, drainage density, and landscape morphology', *Water Resources Research*, **34**, 2751–2764.
Wells, S. G., Dohrenwend, J. C., McFadden, L. D., Turrin, B. D. and Mahrer, K. D. 1985. 'Late Cenozoic landsurface evolution on lava flow surface of the Cima volcanic field, Mojave Desert, California', *Geological Society of America Bulletin*, **96**, 1518–1529.

